Mechanism and Machine Theory 48 (2012) 62–80

Contents lists available at SciVerse ScienceDirect

Mechanism and Machine Theory

journal homepage: www.elsevier.com/locate/mechmt

Static balancing of a four-bar linkage and its cognates

Sangamesh R. Deepak *, G.K. Ananthasuresh

Department of Mechanical Engineering, Indian Institute of Science, Bangalore, India

ARTICLE INFO

Article history:
Received 7 October 2009
Received in revised form 27 May 2011
Accepted 18 September 2011
Available online 8 November 2011

Keywords:
Static balancing
Spring load compensation
Zero-free-length spring
Roberts–Chebyshev cognate theorem

ABSTRACT

Motivated by the need to statically balance the inherent elastic forces in linkages, this paper presents three techniques to statically balance a four-bar linkage loaded by a zero-free-length spring attached between its coupler point and an anchor point on the ground. The number of auxiliary links and balancing springs required for the three techniques is less than or equal to that of the only technique currently in the literature. One of the three techniques does not require auxiliary links. In these techniques, the set of values for the spring constants and the ground-anchor point of the balancing springs can vary over a one-parameter family. Thrice as many balancing choices are available when the cognates are considered. The ensuing numerous options enable a user to choose the most practical solution. To facilitate the evaluation of the balancing choices for all the cognates, Roberts–Chebyshev cognate theorem is extended to statically balanced four-bar linkages.

1. Introduction

A linkage is statically balanced if it is in static equilibrium in its every configuration. Static balancing a linkage under gravity load has received wide attention. Counterweight balancing is known for a long time whereas balancing by adding springs is relatively recent. For example, [13] presented static balancing of a rotatable body by adding springs. [17] discussed balancing of spatial linkages, in particular a two degree-of-freedom serial linkage with revolute joints whose axes intersect perpendicularly. Extending the work of [11] and [12], [14] gave general methods to statically balance gravity forces in multi-link linkages having revolute joints or revolute-slider consecutive pair of joints. Common features of all these methods are: *(i)* the use of *zero-free-length springs* as gravity-compensating elements, *(ii)* the use of auxiliary links, and *(iii)* the presence of only lower-kinematic pairs, the most widely used type of joints. While there are methods that use normally available *positive-free-length springs*, they are either approximate techniques, as in [1], or they make use of joints other than lower-kinematic pairs such as cam-pulley (see [16]).

While the need for static balancing against gravity load is well appreciated and well addressed, there are also applications where static balancing against elastic forces is necessary. One such need articulated by [5] is to balance against elastic forces of cosmetic covering in hand prosthesis. More recently, efforts are underway to statically balance against elastic forces in *compliant mechanisms* (see [7] and [2]). Compliant mechanisms utilize elastic deformation to transmit and/or transform force and motion (see [8]). While in hand prosthesis, the system consists of rigid links and joints with elastic load, in compliant mechanisms there are no rigid links. However, some compliant mechanisms can be approximately modeled as rigid link mechanisms with torsional springs and translational springs (see [9, 8, 4]). No methods have been reported for perfect static balancing of torsional-spring-loaded rigid-link mechanisms. As far as perfect static balancing of rigid-body linkages under translational spring loads are concerned, there is only one reported work, which is of [5]. Herder's method also uses the concept of *zero-free-length springs*, which is discussed later in this paper. While such perfect static balancing theories and the methods presented in this paper may

* Corresponding author.
E-mail addresses: sangu.09@gmail.com (S.R. Deepak), suresh@mecheng.iisc.ernet.in (G.K. Ananthasuresh).

0094-114X/$ – see front matter © 2011 Elsevier Ltd. All rights reserved.
doi:10.1016/j.mechmachtheory.2011.09.009

not be directly applicable for compliant mechanisms, they aid in numerical optimization methods used for balancing compliant mechanisms. In fact, in [2], the starting guess in their numerical optimization was motivated by a spring-loaded rigid-link mechanism. Thus, gaining further insights into static-balancing of spring-loaded rigid-link mechanisms is relevant today. This is one of the motivations for the work presented in this paper.

1.1. Zero-free-length springs and Herder's method

Zero-free-length springs, as the name suggests, have zero-free-length, i.e., their end points coincide when the force in the spring is zero.

The difference between a zero-free-length spring and a non-zero-free-length spring is illustrated in Fig. 1. As shown in Fig. 1, the dependence of spring force $\vec{F}$ on the displacement of one end point of the spring with respect to the other is linear in a zero-free-length spring but nonlinear in a non-zero-free length spring even though both zero-free-length springs and non-zero-free-length springs are assumed to be linear. Because of this nonlinearity, perfect balance of linkages with normally available positive-free-length springs has not been possible as illustrated later in Section 2.1. Since springs other than zero-free-length springs have not been shown to be amenable to perfect static balancing, this paper and [6] assume the springs, both loading spring and those added for balancing, to be zero-free-length springs.

While most normal springs are of positive free-length, one can effectively realize zero-free-length springs and negative-free-length springs using normal springs, as discussed in [13], and [6]. If the load spring is of positive free-length, then before applying Herder's method or the static balancing techniques presented in this paper, one could add a negative free-length spring in parallel to the load spring so that the net effect of the two is a zero-free-length spring. Thus, Herder's method and the methods of this paper can handle any linear tension or compression load springs. Here onwards, unless stated otherwise, all the springs are of zero free-length with linear and positive force-displacement relation.

[5] gave a method to statically balance a four-bar linkage loaded with zero-free-length spring at its coupler point as shown in Fig. 2a. The method involves addition of two auxiliary links and two zero-free-length springs as shown in Fig. 2b. In this paper, we take a different approach to the same problem and give three different techniques to statically balance the linkage. One of the techniques distinguishes itself from the others in that it does not require auxiliary links but only two balancing zero-free-length springs.

1.2. New static balancing methods

Among the three techniques that are presented in this paper, two are new and the remaining is partly new. The first technique that we present requires one balancing spring and two auxiliary links. It is generic in nature and the balancing parameters (i.e., spring constant and anchor point of balancing springs) are not constrained by the linkage parameters (i.e., the location of the joints). Balancing parameters of the remaining two techniques are dependent on the linkage parameters, and both techniques require two balancing springs. While the second technique does not require any auxiliary link, the third technique requires two

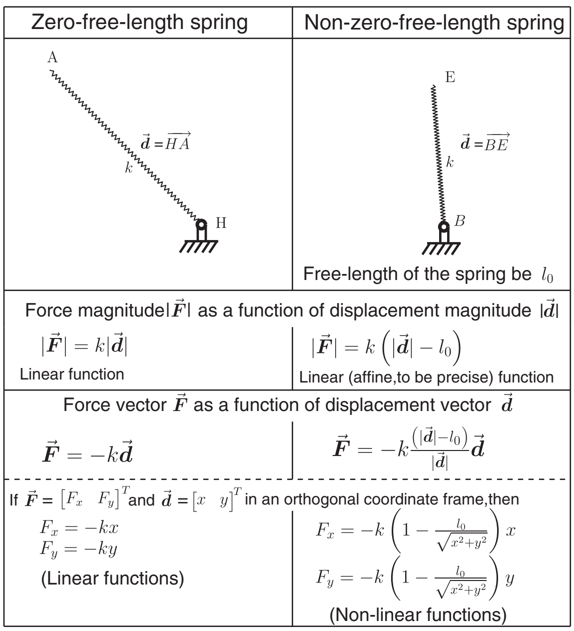

Fig. 1. Difference between zero-free-length and non-zero-free-length springs.

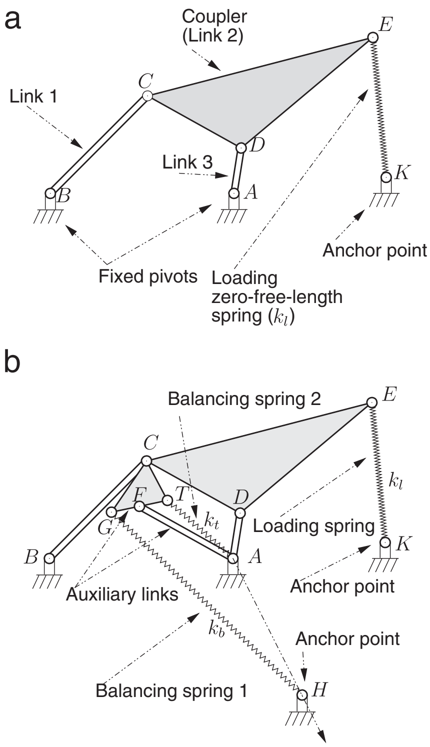

Fig. 2. (a) A four-bar linkage loaded with a zero-free-length spring attached between its coupler point and a fixed anchor point, (b) The four-bar linkage that is statically balanced by addition of two links and two springs using Herder's method.

auxiliary links. Furthermore, the third technique can be applied in two different ways. The balancing solution in one of those ways matches the Herder's solution whereas the remaining one is new. Given a four-bar linkage and a static balancing technique, all the balancing parameters are not unique. For example, in Fig. 2b, the geometry of the auxiliary links and connection points *G*, *E*, and *T* are unique but the anchor point *H* can lie anywhere on a straight line, and the spring constants of the balancing springs are functions of the position of *H*. The non-unique balancing parameters are the same for techniques 2 and 3 and they are:

- Anchor point *H* of balancing spring 1, and
- Spring constants k_b and k_t of balancing springs 1 and 2, respectively.

It is later shown that the set of all possible values for $\{H, k_b, k_t\}$ that ensures static balance is a one-parameter family.

It may be noted that in spite of the reduction or elimination of auxiliary links and balancing springs, a user may find it difficult to satisfy practical constraints. Therefore, additional solutions offered by the cognates could be helpful to choose the most practical solution.

1.3. Static balancing parameters and cognates

A loaded four-bar linkage essentially takes a zero-free-length spring along its coupler curve. In a more general design problem, a zero-free-length spring and the path along which it should be taken are specified, and a designer has to design a four-bar linkage having a coupler curve matching the specified path and also statically balance the four-bar linkage so that the load spring can be moved around the specified path effortlessly. Since the *cognates* of a four-bar linkage have the same coupler curve, all the three cognates enter into the design space. Hence, the designer would have to evaluate the one-parameter family of balancing parameters of a technique on all the cognates. We now present a result which would help the designer to visualize balancing parameters of the other cognates while the balancing parameters of one of the cognates is being evaluated.

If (H_1, k_{b_1}, k_{t_1}), (H_2, k_{b_2}, k_{t_2}), (H_3, k_{b_3}, k_{t_3}), are the balancing variables for the three cognates, then the set $\{(H_1, k_{b_1}, k_{t_1}), (H_2, k_{b_2}, k_{t_2}), (H_3, k_{b_3}, k_{t_3})\}$ is a triplet of one-parameter families. In this paper, a new parameter parametrizing this triplet and having the following features is derived:

1. For any value of the new parameter, the triangle $\triangle H_1H_2H_3$ is similar to the cognate triangle. As the parameter varies, this triangle scales and rotates about a point named as the *focal pivot*.
2. Ratio $k_{b_1} : k_{b_2} : k_{b_3}$ is the same for any value of the new parameter.

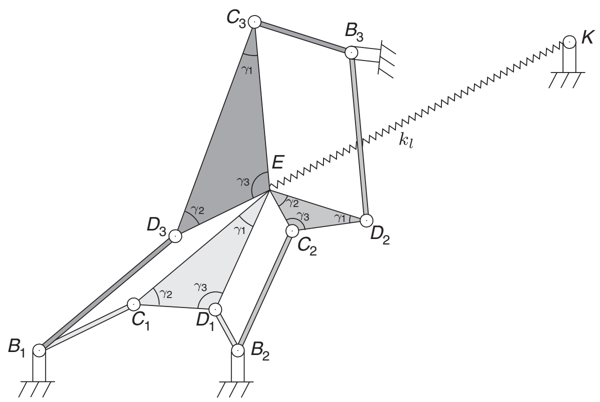

Fig. 3. The cognates of a four-bar mechanism taking a load spring along their common coupler curve.

3. The focal pivot and the ratio $k_{b_1}:k_{b_2}:k_{b_3}$ can be geometrically obtained from the knowledge of the cognate triangle and the ground anchor point of the loading spring.

This result may be viewed as an extension of Roberts–Chebyshev cognate theorem to static balancing.

Roberts–Chebyshev's theorem (see, for example, [10]) says that for a given four-bar linkage and a coupler point on it, one can find two more four-bar linkages and coupler points on them (see Fig. 3) such that the coupler points of all the three trace the same path. The three four-bar linkages are called the *cognates*. The three cognate four-bar linkages in Fig. 3 are — $B_1C_1D_1B_2$, $B_2C_2D_2B_3$, and $B_3C_3D_3B_1$. In the configuration shown, the coupler points of all the three linkages are coincident at E. It is these points which trace the same path. The triangles $B_1B_2B_3$, C_1D_1E, EC_2D_2, and D_3EC_3 are all similar to each other. The triangle formed by the fixed pivots of the cognates (in Fig. 3, it is triangle $B_1B_2B_3$) is called the *cognate triangle*. The ratio of the sides of this triangle appears in many interesting properties of cognates; see [10], for example.

1.4. Organization of the paper

In Section 2, the three techniques for static balancing of a four-bar linkage are presented. In Section 2.3, a prototype of one of the three techniques that doesn't require auxiliary links is described. In Section 3 the extension of Roberts–Chebyshev cognate theorem to static balancing is presented. In Section 4, application of the techniques presented in this paper to gravity loads, 2R linkages and slider crank linkages is discussed. Concluding remarks are in Section 5.

2. Static balancing of a four-bar linkage

In this section, the preliminary concepts used in static balancing of a four-bar linkage are explained first. Detailed discussion on these preliminaries could be found in [6]. After the preliminaries, the three techniques of static balancing a spring-loaded four-bar linkage are described.

2.1. Preliminaries

Some of the simple statically balanced linkages considered in [6] are shown in Figs. 4, 6, and 7.

Shown in Fig. 4 is the simplest of the basic spring balancers described by [6]. When $\overrightarrow{AN} = -\overrightarrow{AP}$, the linkage is statically balanced because the net force at point D, i.e., $2k\overrightarrow{DA}$, is always pointing towards point A for any φ resulting in zero moment of the lever about A.

As a matter of curiosity, let us replace zero-free-length springs in Fig. 4 with non-zero-free-length springs as shown in Fig. 5. The condition for cancelation of horizontal forces becomes $-\frac{l_1-l_0}{l_1}k\overrightarrow{AP} = \frac{l_2-l_0}{l_2}k\overrightarrow{AN}$. Unlike for zero-free-length springs, the balancing condition is not independent of φ, and the condition can only be satisfied for finite values of φ but not for any φ.

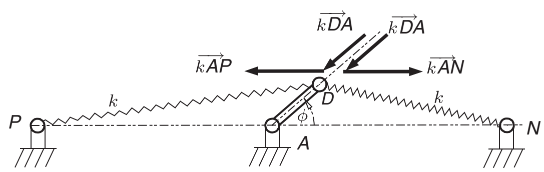

Fig. 4. Basic spring force balancer.

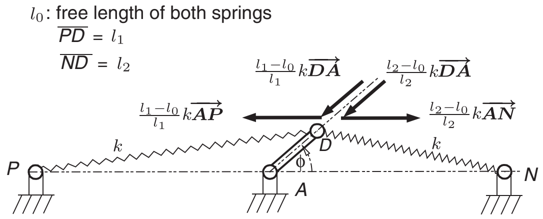

Fig. 5. Zero-free-length springs replaced by normal springs.

Fig. 6 shows a parallelogram linkage, *ADEN*, with two springs diagonally attached between the joints. It may be verified that for the same φ, the potential energy of this system is the same as that in Fig. 4. If one is statically balanced, so is the other.

Fig. 7 shows again a parallelogram linkage but having two degrees of freedom. For the same φ, the potential energy of this system is the same as that in Fig. 6. If one is statically balanced, so is the other.

2.1.1. Composition of springs

In [6], a useful concept of composing two zero-free-length springs into an equivalent one is presented. By referring to Fig. 8, suppose that there is a spring with one end anchored at *A* and the other end at a moving point *E*. Also suppose that we desire the spring to be anchored at point *D* rather than at *A*, but modification of the spring is not allowed. In such a case, another spring of spring constant, say k_2, is connected between point *E* and a point on the ground, say *B*, such that $k_1\overrightarrow{DA} = -k_2\,\overrightarrow{DB}$. When the forces at *E* are resolved along *AD* and *DE*, it can be noticed that forces along *AD* always cancel out and the net force is

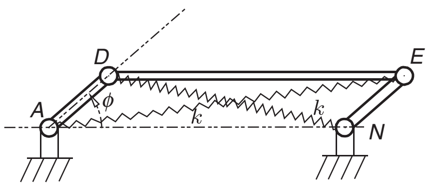

Fig. 6. Balanced parallelogram.

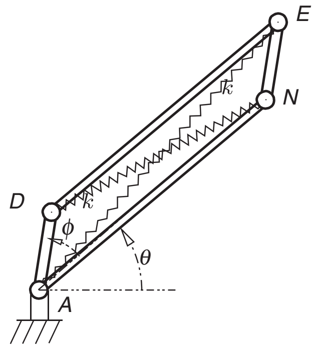

Fig. 7. Balanced two degree of freedom parallelogram linkage.

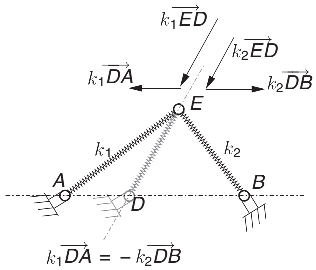

Fig. 8. Composition of two zero-length-spring into an equivalent one. The equivalent spring between *E* and *D* is shown in gray color.

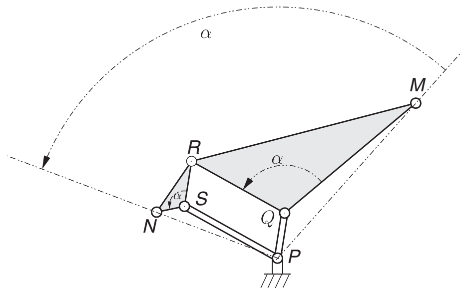

Fig. 9. A plagiograph or a skew pantograph linkage.

$(k_1+k_2)\overrightarrow{ED}$. The same force is obtained if there were to be a spring of spring constant (k_1+k_2) anchored at D and the other end at E. Hence the net effect or *composition* of the two springs anchored at A and B is a virtual spring anchored at D. This is an important concept for the techniques presented in this paper.

2.1.2. Plagiograph

In a plagiograph linkage, the path traced at the output point is a scaled and rotated replica of the path traced at the input point. If the linkage shown in Fig. 9 satisfies the following conditions:

1. $\overline{PQ} = \overline{SR}$ and $\overline{PS} = \overline{QR}$ so that $PQRS$ is a parallelogram,
2. $\angle RQM = \angle NSR$ (this angle is labeled as α) and $\frac{RQ}{MQ} = \frac{NS}{RS}$ (this ratio is labeled as m) so that $\triangle NSR$ is similar to $\triangle RQM$,

then the linkage is called a plagiograph or a skew pantograph. It has the following property: output point N follows the input point M through a scaling and rotation transformation about point P with the scale factor and the rotation angle being m and α. That is,

$$\overrightarrow{PN} = mR_a\left(\overrightarrow{PM}\right) \tag{1}$$

where, R_a is the rotation operator which operates on a planar vector to rotate it by the angle α.

The point, P, about which scaling and rotation transformation happens is referred as the base pivot of the plagiograph. A detailed treatment of plagiographs can be found in [3] and [15].

2.2. Static balancing a given spring-loaded four-bar linkage

Consider a four-bar linkage loaded by a zero-free length spring at its coupler point as shown in Fig. 1.

Before adding auxiliary links and additional springs to balance it, let us see if there is a possibility of it being in static balance as such. Fig. 10 shows the coupler curve traced by point E. If the linkage has to be in equilibrium at every configuration, then the potential energy of the spring has to be the same for every configuration. This is possible only when every point of the coupler curve is at a constant distance from K, i.e., when the coupler curve is a circle centered at K. In general this is not true except in extreme cases such as when E coincides with D (or C) and K coincides with A (or B).

Next, various possibilities of static balancing a four-bar linkage by adding auxiliary links and springs are considered. Only those possibilities where the number of additional balancing springs and auxiliary links is less than or equal to that of [5] are explained. As can be seen in Fig. 1, [5] used two auxiliary links and two balancing springs.

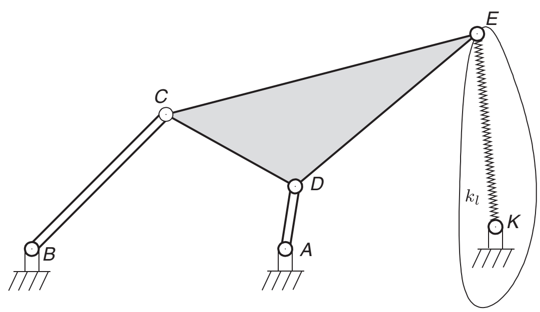

Fig. 10. A four-bar linkage with an anchored load spring attached to its coupler point.

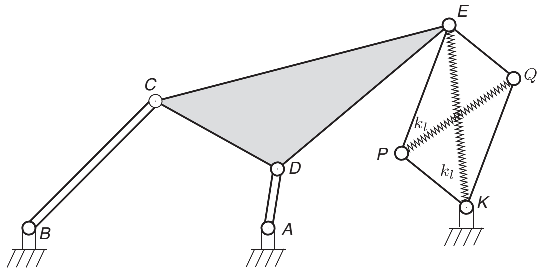

Fig. 11. A balanced parallelogram on the load spring.

2.2.1. Technique 1

Motivated by the observation in Fig. 7, the four-bar linkage can be balanced by creating a balanced parallelogram as shown in Fig. 11. Here, four auxiliary links and one balancing spring are used. But the number of auxiliary links can be reduced to two.

2.2.1.1. Reducing the number of auxiliary links. As shown in Fig. 12, if *T* is a point on the (extended) link *EP* such that $\overrightarrow{EP} = \overrightarrow{PT}$, then *TKQP* forms a parallelogram. Relocation of the spring between *P* and *Q* to be between *T* and *K* does not change its potential energy and hence static balance is undisturbed. The advantage of the relocation is that the two auxiliary links *KQ* and *QE* are unnecessary. This way of balancing is this paper's technique 1 to statically balance a four-bar linkage.

The characteristics of technique 1 can be summarized as follows:

1. This way of balancing does not induce any load in any of the links making up the four-bar linkage.
2. The balancing variables are l_1, and l_2, i.e., lengths of *PE* and *PK*, as shown in Fig. 12. l_1 and l_2 can be of any convenient values.

2.2.2. Technique 2

Instead of adding four links to make up a parallelogram as in Fig. 11, addition of only two auxiliary links is necessary if links *ED* and *DA* are used to form the parallelogram as shown in Fig. 13. This parallelogram can balance a spring connected between its opposite vertices. While the load spring is not between its opposite vertices, another spring (labeled as balancing spring 1) is

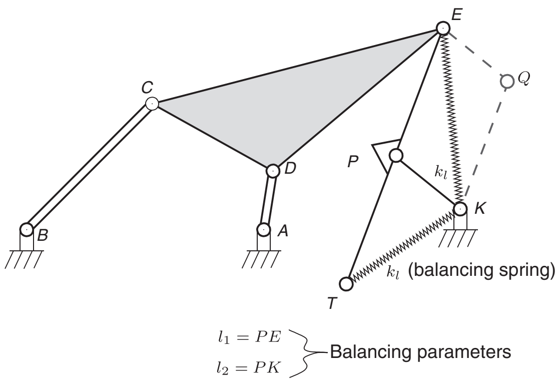

Fig. 12. Technique 1: static balancing with two auxiliary links and one balancing spring.

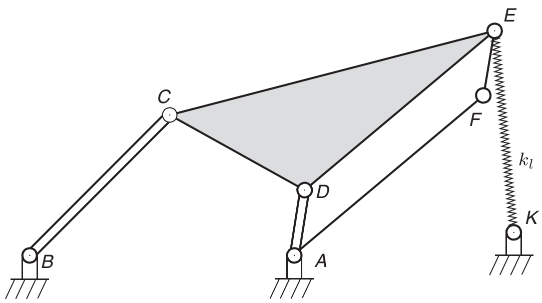

Fig. 13. Forming a parallelogram using two auxiliary links.

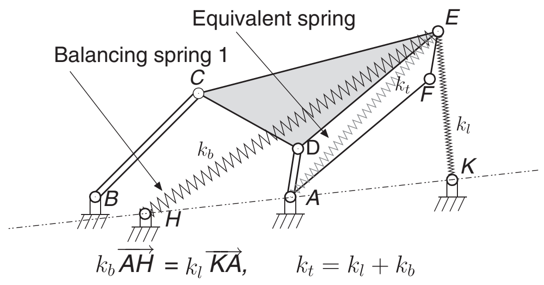

Fig. 14. An equivalent spring between opposite vertices of the parallelogram *AFED*.

added so that the resultant of its composition with the load spring is between the opposite vertices of the parallelogram, as shown in Fig. 14. Recall the composition property of springs noted in Section 2.1.1.

The equivalent spring between *A* and *E* in Fig. 14 is balanced by adding another spring (labeled as balancing spring 2) across the other two opposite vertices of the parallelogram as shown in Fig. 15. Thus, the equivalent spring and balancing spring 2 are in static balance. Equivalently, the load spring, balancing spring 1 and balancing spring 2 are in static balance. With this, the linkage is in static balance with two auxiliary links and two balancing springs. The auxiliary links can be eliminated as explained next.

As shown in Fig. 16, if *T* is a point on link *DE* (extended if necessary) satisfying $\overrightarrow{ED} = \overrightarrow{DT}$, then *AFDT* is always a parallelogram and *DF* = *TA*. Hence, relocation of the spring between *D* and *F* in Fig. 15 to be between *T* and *A* as in Fig. 16 does not change its potential energy. Consequently, the static balance is also undisturbed. Furthermore, the auxiliary links *AF* and *FE* are no longer required. This way of balancing shown in Fig. 16, requiring two balancing spring but no auxiliary link, is the second technique of this paper to balance a four-bar linkage.

This technique has two options. In Fig. 13, a parallelogram was completed out of links *AD* and *DE*. One could have completed the parallelogram out of links *BC* and *CE* as well and proceed in a similar manner. We say that the balanced parallelogram is based at *A* in the former case and based at *B* in the latter case.

Among the balancing parameters of this technique, the anchor point of balancing spring 2 is always one of the fixed pivots of the four-bar linkage. The remaining balancing parameters: *(i) H*, the anchor point of balancing spring 1, *(ii)* k_b, the spring constant of balancing spring 1, and *(iii)* k_t, the spring constant of balancing spring 2, have to be solved from the equations included in

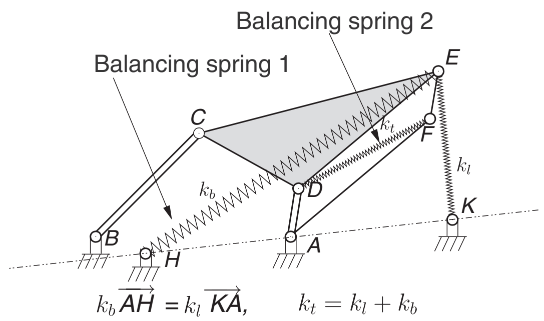

Fig. 15. Adding balancing spring 2 across opposite sides of the parallelogram to balance the load spring and balancing spring 1.

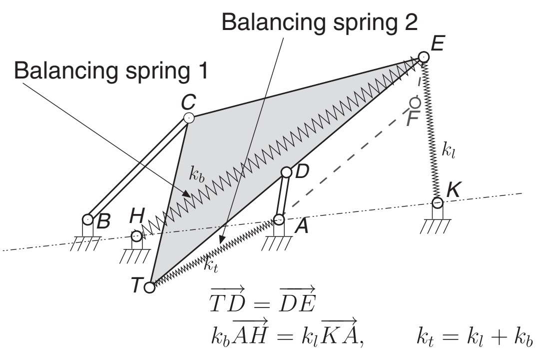

Fig. 16. Option 2 for balancing the four-bar linkage without auxiliary links.

Fig. 16. Those equations can be rewritten in a general form so that they are applicable to both the options of this technique. If W is where the balanced parallelogram is based (i.e., W is A or B) and K is the anchor point of load spring, then

$$k_b \overrightarrow{WH} = k_l \overrightarrow{KW} \quad (2)$$

$$k_b = k_l \frac{KW}{WH} \left(\text{positive if } \overrightarrow{WH} \text{ is along } \overrightarrow{KW}, \text{ and negative otherwise}\right) \quad (3)$$

$$k_t = k_b + k_l. \quad (4)$$

Eq. (2) says that H has to lie on a line starting from W and along the direction of $\overrightarrow{KW}$. The line is called the straight-line locus of H. Once a point on this line is chosen as H, k_b and k_t get determined as per Eqs. (3) and (4). Thus the set of solutions to (H, k_b, k_t) is a one-parameter family.

2.2.3. Technique 3

As mentioned earlier, the only known method in literature to statically balance a spring-loaded four-bar linkage was described by [5]. In the work of [5], a plagiograph is first statically balanced and then it is modified to obtain a balanced four-bar linkage with two auxiliary links and two balancing springs as shown in Fig. 2b. It is now shown that the balancing arrangement obtained by [5] can also be obtained by combining technique 2 of this paper with the concept of plagiograph. This later approach is technique 3 of this paper. Whereas technique 3 provides four options, the approach of [5] provides only two of these options. Technique 3 and its options are described next.

In technique 2, balancing spring 1 and the loading spring were connected to the coupler at the same point, coupler point E. If the coupler point is not accessible to balancing spring 1, then another point to anchor the spring has to be found. It is also desirable that the motion of the other point is related to the coupler point. By taking a cue from Section 2.1.2, a plagiograph can be

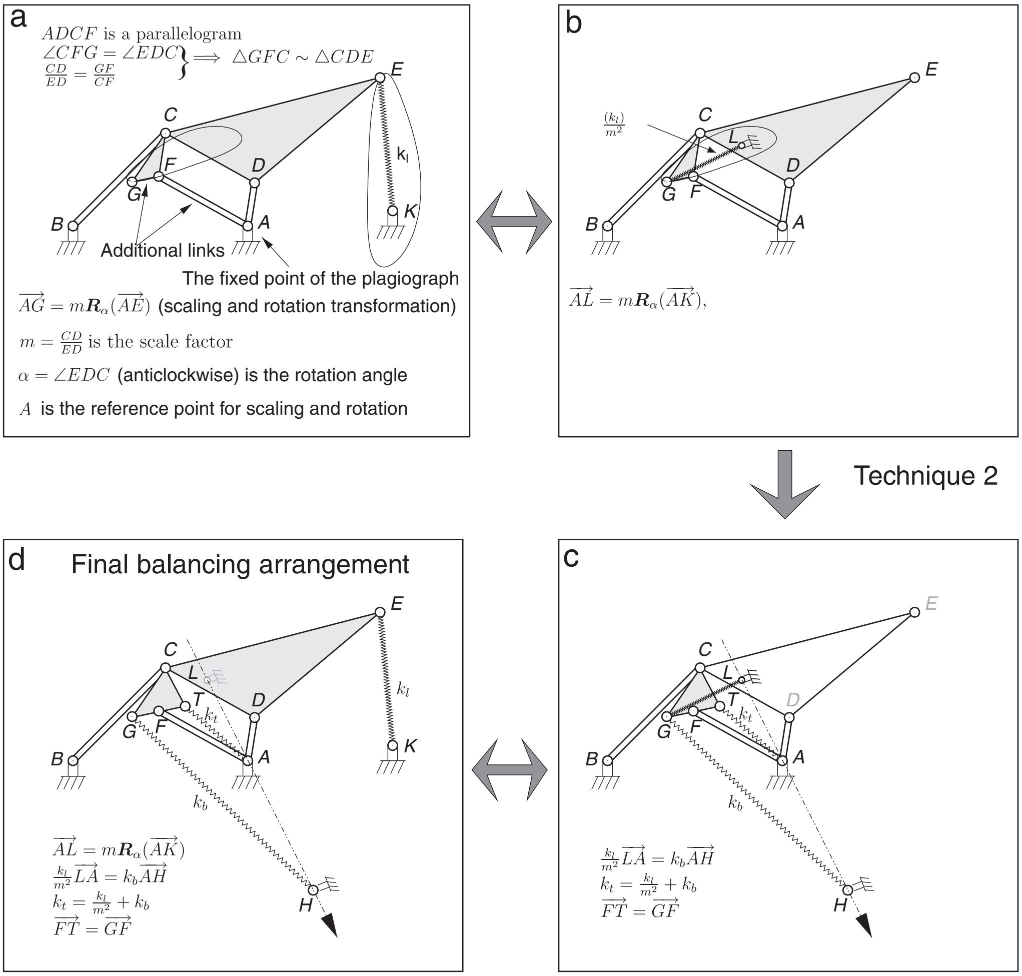

Fig. 17. Technique 3 for statically balancing a four-bar linkage.

completed out of two links of the given four-bar linkage, as shown in Fig. 17a so that point G follows a scaled and rotated locus of coupler point E.

Whatever scaling and rotation transformation of point E that point G follows, the same transformation is applied to point K to obtain point L, i.e.,$\overrightarrow{AL} = mR_a\left(\overrightarrow{AK}\right)$, as shown in Fig. 17b. If a spring is attached between point L and point G, as in Fig. 17b, then the spring is a scaled (by factor m) and rotated copy of the load spring in Fig. 17a. Further, if the spring constant of the spring in Fig. 17b is $\frac{1}{m^2}$ times the spring constant of the load spring, i.e., $\frac{k_l}{m^2}$, then its potential energy $\frac{k_l}{2m^2}(LG)^2 = \frac{k_l}{2m^2}(m(KE))^2 = \frac{k_l}{2}(KE)^2$ is the same as that of the load spring. Therefore, the potential energy of the spring loads in Fig. 17a and b are the same. As a consequence of this, any extra spring addition that balances the spring load in Fig. 17b would also balance the spring load in Fig. 17a.

In Fig. 17b, one may think of links BC, CF, and FA to constitute a four-bar linkage loaded with a spring at its coupler point G. Application of technique 2 of static balancing to this spring-loaded linkage leads to addition of two extra spring, as shown in Fig. 17c. The same two springs would statically balance the spring load of Fig. 17a also.

Balancing the given spring load of Fig. 17a by adding the balancing springs of Fig. 17c, as shown in Fig. 17d, is the third technique to balance a spring-loaded four-bar linkage. It may be noted in Fig. 17d that none of the balancing springs are connected to coupler point E.

When the four-bar linkage of Fig. 17b was balanced using technique 2, there were two options: balanced parallelogram based at A or based at B (see Section 2.2.2 describing technique 2).

Furthermore, when a plagiograph was completed out of the four-bar linkage in Fig. 17a, the base pivot of the plagiograph was at A. We can also complete a plagiograph out of the same four-bar linkage so that the base pivot is at B, as shown in Fig. 18. Thus, we have $2\times2=4$ options, i.e., the base pivot of plagiograph at A or B, and balanced parallelogram based at A or B. In the technique of [5], the base pivots of both plagiograph and balanced parallelogram always coincide. Therefore only two of the above four options are derivable from the technique of [5].

The equations provided in Fig. 17d are necessary to solve for the ground anchor-point of balancing spring 1 (H), the spring constant of balancing spring 1 (k_b) and the spring constant of balancing spring 2 (k_t). In the equations, point A is the base pivot of both plagiograph and balanced parallelogram. To make the equations applicable to any of the four options of this technique, notations U and W respectively denoting the base pivots of plagiograph and balanced parallelogram are appropriately substituted for A in the equations as follows:

$$\overrightarrow{UL} = mR_\alpha\left(\overrightarrow{UK}\right) \quad \text{(L is the anchor point of the equivalent load spring)} \tag{5}$$

$$\overrightarrow{WH} = \frac{k_l}{m^2 k_b}\overrightarrow{LW} \tag{6}$$

$$k_b = \frac{k_l(LW)}{m^2(WH)} \quad \left(\text{positive if } \overrightarrow{WH} \text{ is along } \overrightarrow{LW}, \text{ negative otherwise}\right) \tag{7}$$

$$k_t = k_b + \frac{k_l}{m^2} \tag{8}$$

m and α in the above equations are found from Fig. 17a or 18 depending on whether U is A or B. Eq. (6) indicates that H can lie anywhere on a line along $\overrightarrow{LW}$ and passing through W. Spring constants k_b and k_t are functions of the position of H on this line, as per Eqs. (7) and (8). Therefore, the set of all solutions for (H, k_b, k_t) is a one-parameter family.

The main features of the three techniques presented in this section as well as Herder's method are summarized in Table 1.

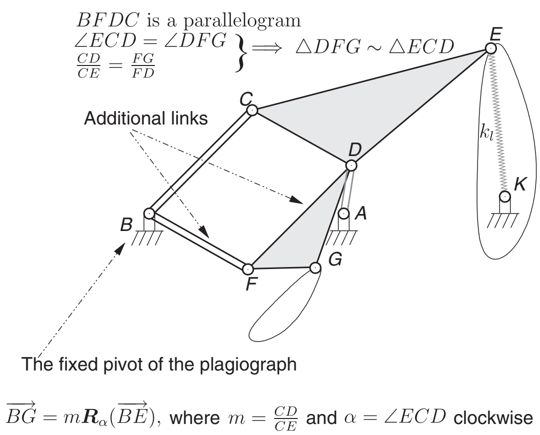

Fig. 18. Plagiograph with base pivot at B.

Table 1
Summary of different techniques to statically balance a spring-loaded four-bar linkage presented in this paper.

	Technique 1	Technique 2	Technique 3	Herder's Technique
Number of Auxiliary Links	2	0	2	2
Number of balancing springs	1	2	2	2
Variable balancing parameters	l_1, l_2	H, k_b, k_t	H, k_b, k_t	H, k_b, k_t
Family of feasible balancing parameters	Two-parameter	One-parameter	One-parameter	One-parameter
Number of options	One	Two	Four	Two

2.3. Prototype with technique 2

A prototype of a spring-loaded four-bar linkage balanced using technique 2 is shown in Fig. 19. The zero-free-length springs used in the prototype were realized using 'pulley and string arrangement' described by [6]. A pulley and string arrangement consists of a normal spring having its one end anchored to the ground and the other end connected to a string. The string passes over a *small* pulley pivoted to the ground, as shown in Fig. 20. The pulley that is assumed to be frictionless and of negligible diameter transmits both tension and deflection of the normal spring. Hence, the portion of the string that has passed over the pulley may be thought as a virtual spring of stiffness the same as the normal spring stiffness. The virtual spring acquires zero-free-length if the arrangement is such that the passed-over length of the string is zero when the tension is zero.

The prototype design is such that the ratio of spring constant of loading spring, balancing spring 1 and balancing spring 2 is 1 : 1 : 2. To realize these three springs, three identical springs were taken. While two spring were used as it is within spring-pulley arrangements, only half the length of the spring was used for the remaining spring, as can be seen in the right hand side of Fig. 20. It may be noted that the anchor points of loading spring and balancing spring 1 on the coupler link are the same. Further, the anchor points of the loading spring and balancing spring 2 on the coupler link are located symmetrically with respect to a revolute joint on the coupler link. It may further be verified that the prototype satisfy Eqs. (2)–(4).

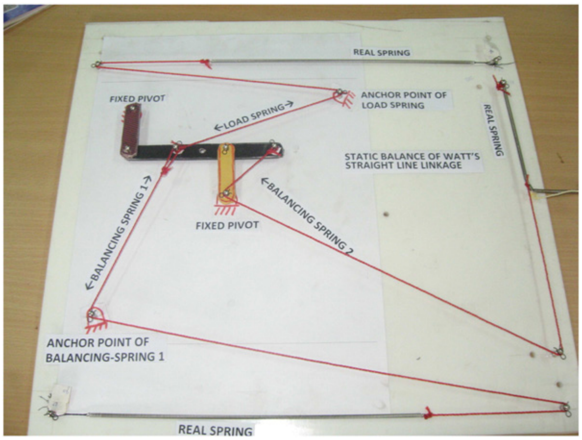

Fig. 19. A prototype of four-bar linkage that is statically balanced using option 2. The four-bar linkage seen in the above figure is a Watt's straight-line mechanism.

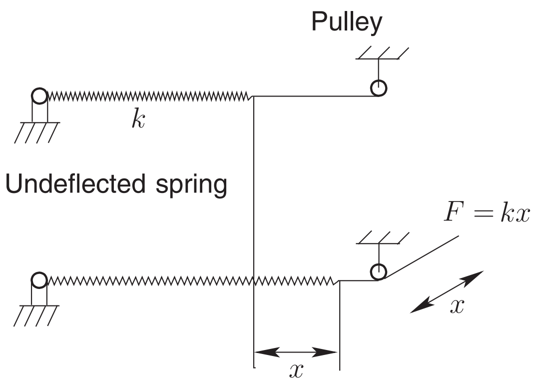

Fig. 20. Realization of a zero-free length spring.

3. Static balancing parameters and the cognates

A designer seeking to statically balance a given spring-loaded four-bar linkage has to evaluate a family of feasible balancing parameters for each of the options under the three techniques (see Table 1) before choosing the one that best meets the design requirements. As was remarked in Section 1.3, a more general design problem would be to design a four-bar linkage that would guide a given load spring along a specified path and then statically balance the linkage so that the load spring can be moved along the path effortlessly. If a four-bar linkage with its coupler curve matching the specified path is found, then by Roberts–Chebyshev cognate theorem, it follows that there are two more four-bar linkages whose coupler curves also match the specified path. In order make the best design choice, the designer has to evaluate feasible balancing parameters of options under techniques 2 and 3 on all the three cognates. This section presents a result which will aid the designer to evaluate these feasible balancing parameters on all the cognates in a unified manner. Evaluation could be for the space occupancy of the balancing arrangements or for the loads that linkages experience. As far as technique 1 is concerned, the balancing parameters can be evaluated independent of the four-bar linkage.

Since three four-bar linkages are considered in this section, the balancing parameters of techniques 2 and 3, such as H, k_b, k_t, W, U, and L, are subscripted with 1, 2, or 3 to correspond to the first, the second or the third cognate. Since all the cognates are evaluated for the same load spring, load-spring-anchor-point K and loading spring-constant k_l are the same for all the cognates. When an option of technique 2 or 3 is applied with a cyclic symmetry on all the cognates, each of (H_1, k_{b_1}, k_{t_1}), (H_2, k_{b_2}, k_{t_2}), and (H_3, k_{b_3}, k_{t_3}) can vary over their respective one-parameter family. Instead of separate parametrizations for the three one parameter families, this section aims to give a single parametrization of the triplet $\{(H_1, k_{b_1}, k_{t_1}), (H_2, k_{b_2}, k_{t_2}), (H_3, k_{b_3}, k_{t_3})\}$ such that the parametrization has cognate related invariants.

Suppose that an option of technique 2 or 3 is applied on all the cognates with a cyclic symmetry. To derive a cognate triangle related parametrization for $\{(H_1, k_{b_1}, k_{t_1}), (H_2, k_{b_2}, k_{t_2}), (H_3, k_{b_3}, k_{t_3})\}$, one should first establish the locus of H_i as well as k_{b_i} and k_{t_i} as a function of position of H_i, for $i = 1, 2, 3$. This is possible only if the constant terms, such as W_i, U_i, m_i, α_i and L_i, in Eqs. (2)–(4) in the case of technique 2 or Eq. (5)–(8) in the case of technique 3 are known. Deduction of these constant terms from the details of the given four-bar linkage was seen in Sections 2.2.2 and 2.2.3. However, Table 2 shows that they can also be deduced from the cognate triangle and the ground-anchor point of the loading spring. Thus, the knowledge of the cognate triangle and the ground-anchor point of the loading spring is sufficient to establish the locus of H_i and the relation between H_i, k_{b_i} and k_{t_i}, for $i = 1, 2, 3$.

Fig. 21a shows the cognate triangle and the ground-anchor point of the loading spring. The sides corresponding to cognates 1, 2 and 3 are labeled as s_1, s_2, and s_3, respectively. If the static balancing option used happens to be the option of technique 3 that has the base point for both plagiograph and balanced parallelogram at the anticlockwise end of s_1, s_2, and s_3, then the loci of H_1, H_2 and H_3, denoted by l_1, l_2 and l_3, are as shown in Fig. 21b. If a different option of the same technique or an option of technique 2 is used, then a different set of loci are obtained, as shown in Fig. 21c and d. Note that for both techniques, the origin for l_1, l_2 and l_3 is one of the vertices of the cognate triangle with a *one–one and onto* relation between the origins and the vertices. Because of this feature, it is now shown that H_1, H_2 and H_3 can be varied along their loci as if they are at the respective vertices of the cognate triangle that is undergoing scaling and rotation transformation about a fixed point. When H_1, H_2 and H_3 are varied as noted above, k_{b_1}, k_{b_2} and k_{b_3} also vary. However, it will be shown that their ratio remains constant. This result follows from a solution given in this paper to a problem in geometry. The problem and its solutions are described next.

3.1. A geometric problem and its solution

Given a triangle and three straight lines originating from its three vertices, find three points on the three lines so that they form a triangle that is similar to the given triangle. With respect to Fig. 22, the problem may be stated as: find points S_a, S_b and S_c on straight-lines a, b and c respectively so that $\triangle S_aS_bS_c$ is similar to $\triangle ABC$.

The method to obtain S_a, S_b and S_c varies for the following three cases, as described next.

Table 2
Deduction of various quantities in Eqs. (2)–(8) from the cognate triangle.

Quantities other than H, k_b and k_t in Eq. (2)–(8):	
K, U, W, m, α, L	
K	Anchor point of loading spring
W	Base pivot of balanced parallelogram ⇒ Coincident with a fixed pivot of the four-bar linkage ⇒ One of the vertices of the *cognate* triangle ∵ Fixed pivots of cognates form the cognate triangle (see Fig. 3)
U	Base of pivot plagiograph ⇒ One of the vertices of the *cognate* triangle (for the same reasons as of W)
m	Ratio of two sides of the coupler triangle (see Figs. 17a and 18) ⇒ Ratio of two sides of the *cognate* triangle ∵ Cognate triangle is similar to coupler triangle (see Fig. 3)
α	An angle of the coupler triangle (see Figs. 17a and 18) ⇒ An angle of the *cognate* triangle (∵ cognate △ ~ coupler △)
L	Anchor point of equivalent of loading spring (see Fig. 17b) Found using the equation $\overrightarrow{UL} = mR_\alpha(\overrightarrow{UK})$. ($U$, m, α and K are as above.)

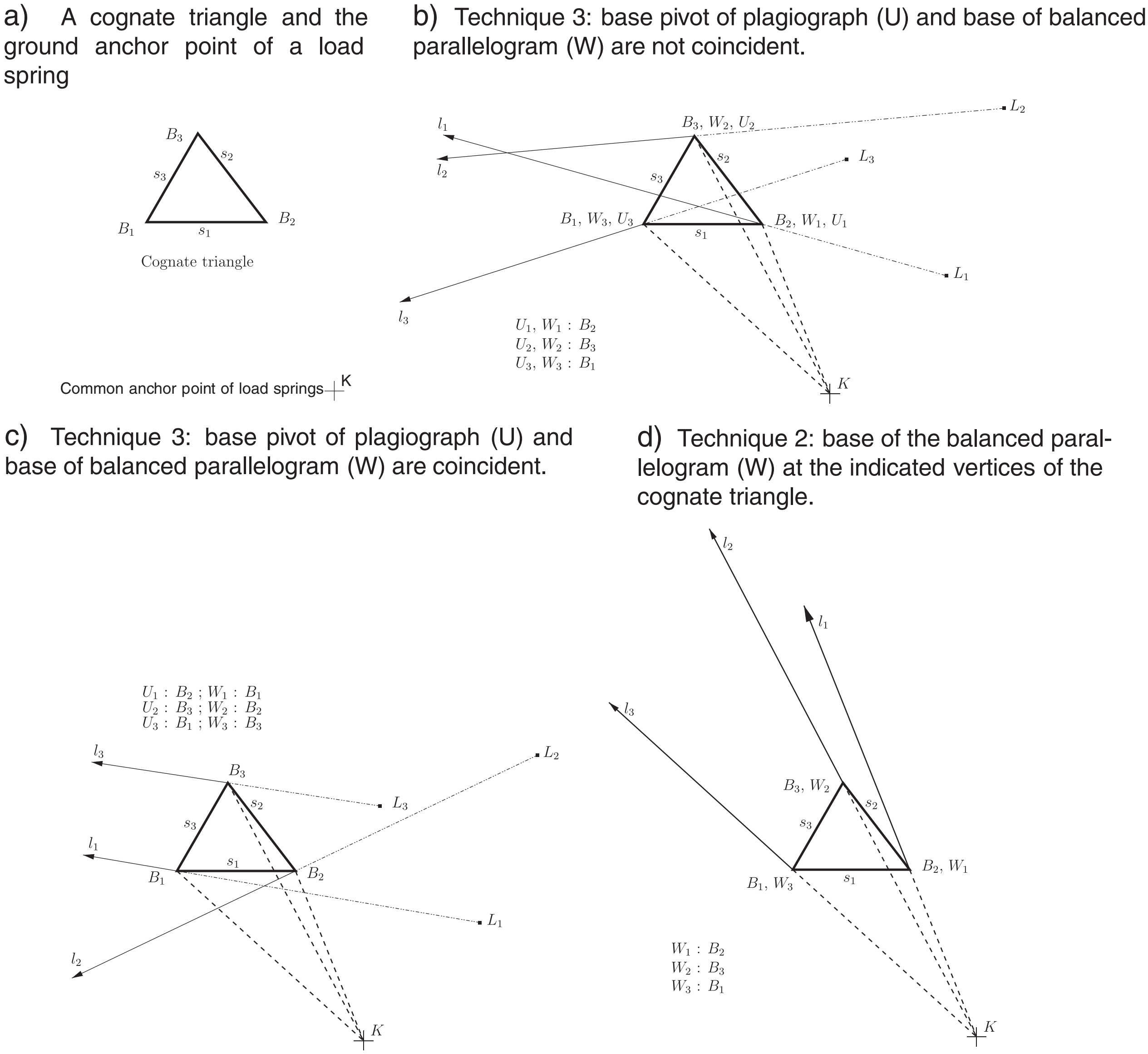

Fig. 21. The locus of anchor point of balancing spring 1 (H) for the three cognates under options of techniques 2 and 3.

3.1.1. Case (i): a, b and c are parallel

S_a, S_b and S_c can be obtained by translating A, B and C along the parallel lines, as shown in Fig. 23, because S_a, S_b and S_c respectively lie on lines a, b and c, and $\triangle S_aS_bS_c$ is congruent to $\triangle ABC$.

3.1.2. Case (ii): a, b and c are concurrent

S_a, S_b and S_c can be obtained by scaling A, B and C about the point of concurrence, as shown in Fig. 24, because S_a, S_b and S_c respectively lie on lines a, b and c, and $\triangle S_aS_bS_c$ is similar to $\triangle ABC$.

3.1.3. Case (iii): a, b, and c are neither parallel nor concurrent

If the geometric problem does not fall under case *(i)* or case *(ii)*, such as the one in Fig. 22, then it falls under case *(iii)*. In this case, it is proved later in Section 3.1.4 that there exists a non-zero angle η such that when lines a, b and c are rotated by the same angle η about points A, B, and C, respectively, the lines become concurrent at a point, as depicted in Fig. 25. The concurrent point is named as *focal pivot*. In Fig. 25 the focal pivot is denoted as P. In order to find a solution to S_a, S_b and S_c, obtain $\triangle A_1B_1C_1$ that is the rotated copy of $\triangle ABC$ about point P by some angle δ, as shown in Fig. 26. If the respective intersection points of lines PA_1, PB_1, and PC_1 with lines a, b, and c are A_2, B_2, and C_2, as shown in Fig. 26, then it is proved in the following paragraph that $\triangle A_2B_2C_2$ is similar to $\triangle ABC$.

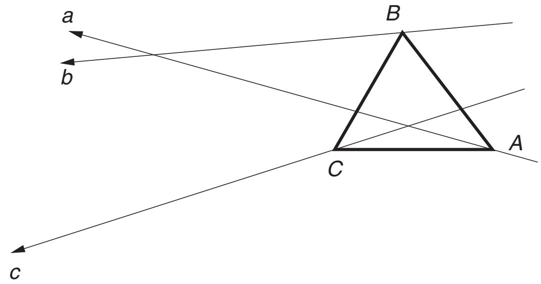

Fig. 22. Find a triangle similar to $\triangle ABC$ with corresponding vertices on the same line.

Points A_2, B_2 and C_2 form a solution to S_a, S_b and S_c because $\triangle A_2B_2C_2$ and $\triangle ABC$ are similar, and by definition, points A_2, B_2 and C_2 lie on lines a, b and c, respectively. Different values of angle δ leads to different solutions.

Proof of similarity of $\triangle A_2B_2C_2$ and $\triangle ABC$. $\triangle A_2PA$, $\triangle B_2PB$ and $\triangle C_2PC$ are similar to each other since angles δ and η are common to all of them. Hence

$$\frac{PA_2}{PA} = \frac{PB_2}{PB} = \frac{PC_2}{PC} \tag{9}$$

Substitution of $PA = PA_1$, $PB = PB_1$ and $PC = PC_1$ ($\triangle A_1B_1C_1$ is a rotated copy of $\triangle ABC$ about P) in Eq. (9) leads to $\frac{PA_2}{PA_1} = \frac{PB_2}{PB_1} = \frac{PC_2}{PC_1}$. $\frac{PA_2}{PA_1} = \frac{PB_2}{PB_1} = \frac{PC_2}{PC_1}$ implies that $\triangle A_2B_2C_2$ is a scaled copy of $\triangle A_1B_1C_1$ (about P). In turn $\triangle A_1B_1C_1$ is a rotated copy of $\triangle ABC$ (about P). Hence, $\triangle A_2B_2C_2$ is similar to $\triangle ABC$, and it can be visualized as a rotation and scaling transformation of $\triangle ABC$ about the focal pivot P.

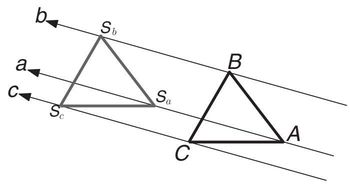

Fig. 23. Finding S_a, S_b, and S_c in case *(i)*.

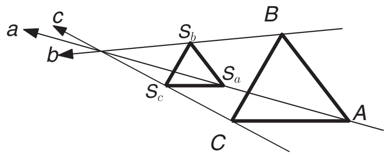

Fig. 24. Finding S_a, S_b, and S_c in case *(ii)*.

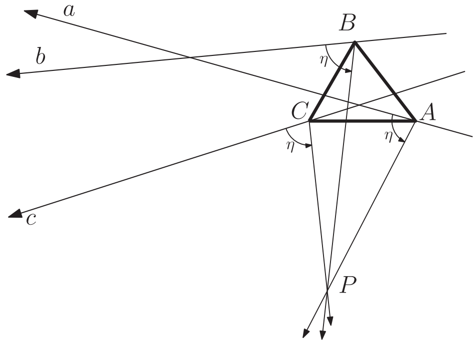

Fig. 25. Description of focal pivot.

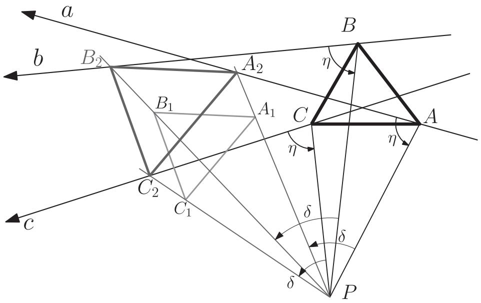

Fig. 26. Points A_2, B_2 and C_2 form a solution to S_a, S_b and S_c.

3.1.4. Finding the focal pivot

Let lines a, b and c be rotated by the same angle, say β, about points A, B and C, respectively. If for some β, the three lines become concurrent, then by definition, $\beta=\eta$, and the point of concurrence is the focal pivot. If $I_{a,b}$ is the intersection point of lines a and b, and $I_{c,a}$ is the intersection point of lines c and a, then at the concurrence, $I_{a,b}$ and $I_{c,a}$ meet. $I_{c,a}$ and $I_{a,b}$ can meet only at the intersection of paths that $I_{a,b}$ and $I_{c,a}$ trace when angle β is varied continuously.

The path traced by $I_{a,b}$ is a circle passing through A, B and the original position of $I_{a,b}$ (see the theorem in Appendix B).

Similarly, the locus of $I_{c,a}$ is a circle passing through C, A and the original position of $I_{c,a}$. The two loci are shown in Fig. 27. Locating the focal pivots in all the possible types of intersection between the loci is addressed as follows.

- *$I_{a,b}$, or $I_{c,a}$ will not exist when the a and b, or c and a are parallel and hence the $I_{a,b}$ and $I_{c,a}$ circles cannot be drawn*: Finding the focal pivot is necessary only in case *(iii)*, where all three of a, b and c are not parallel to each other. Hence, it is possible to find at least two pairs among a, b and c that are not parallel to each other. Those pairs may be taken as $\{a,b\}$ and $\{c,a\}$, for which $I_{a,b}$ and $I_{c,a}$ exists.
- *$I_{a,b}$ circle and $I_{c,a}$ circle are coincident*: It is shown in Appendix A.1 that if $I_{a,b}$ circle and $I_{c,a}$ circle are coincident, then a, b and c before rotation (at $\beta=0$) have to be concurrent. Concurrency at $\beta=0$ means that the problem falls under case *(ii)*. Since the procedure to find the focal pivot is used only for case *(iii)*, the possibility of coincidence of $I_{a,b}$ and $I_{c,a}$ circles does not arise.
- *$I_{a,b}$ circle and $I_{c,a}$ circle intersect at two distinct points*: This is the generic possibility and is illustrated in Fig. 27. One of the intersection points is always A. The other intersection point is denoted as M. In Appendix A.2, it is shown that if rotation angle β is such that $I_{a,b}$ is at M, then for the same β, $I_{c,a}$ is also at M. On the other hand, if β is such that $I_{a,b}$ is at A, then for the same β, $I_{c,a}$ cannot be at A. Hence, it can be concluded that M is the one and only focal pivot.
- *$I_{a,b}$ circle and $I_{c,a}$ circle touch each other at a single point*: This is just a limiting case of two distinct intersection points A and M of the previous possibility merging into one. Here also, M, which coincides with A, is the only focal pivot.

Thus, to find the focal pivot for case *(iii)*, by assuming that non-parallel pair of lines are $\{a,b\}$ and $\{c,a\}$, one should draw two circles: one passing through A, B and $I_{a,b}$ (at $\beta=0$) and the other passing through C, A, $I_{c,a}$ (at $\beta=0$). The two circles either intersect at two distinct points: M and A, or touch at the point A. In the former case, the focal pivot is M and in the later case it is A.

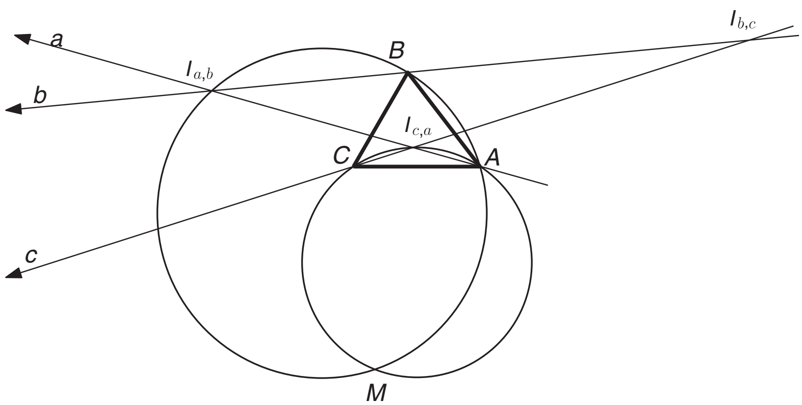

Fig. 27. Geometric construction to find the focal pivot.

The common properties of solution to S_a, S_b and S_c in all the possible cases presented in Sections 3.1.1, 3.1.2 and 3.1.3 are summarized below.

- The set of possibilities for S_a, S_b and S_c constitute a one-parameter set. A convenient parameter parametrizing the set in case *(i)* is the translation, in case *(ii)* is the scale factor, and in case *(iii)* is the rotation angle δ.
- The ratio $AS_a : BS_b : CS_c$ is the same throughout the one-parameter set even though AS_a, BS_b and CS_c themselves vary over the set. The ratio is $1:1:1$ in case *(i)*, $PA:PB:PC$ in case *(ii)*, and again $PA:PB:PC$ in case *(iii)* (see Eq. (9) where A_2, B_2 and C_2 are solutions to S_a, S_b and S_c).

These properties are now applied to the cognate triangle and loci l_1, l_2, and l_3, as described next.

3.2. A parametrization with cognate-triangle-related invariants

The solutions given in Section 3.1 are now applied to the cognate triangle and loci of H shown in Fig. 21, by taking A, B, C, a, b, c, S_a, S_b, S_c as W_1, W_2, W_3 (the vertices of the cognate triangle), l_1, l_2, l_3, H_1, H_2, H_3, respectively. Then properties at the end of Section 3.1, take the following form:

There is a one-parameter parametrization of the balancing variables of the three cognates where

- $\triangle H_1H_2H_3$ is similar to $\triangle W_1W_2W_3$ (the cognate triangle), and
- the ratio $W_1H_1 : W_2H_2 : W_3H_3 = W_1P : W_2P : W_3P$ or $1:1:1$ is the same for the entire one parameter set of possibilities.

The second property is used in Table 3 to rewrite the ratio of spring constants of balancing spring 1 of the three cognates. It is seen that the ratio involves only constants. Hence, the ratio itself is invariant for this one-parameter set. It may further be noted that all these constants are derivable just with the knowledge of the cognate triangle and the location of the ground-anchor point of the loading spring. With this follows the final result of this section: when an option of technique 2 or 3 is applied on all the cognates, the family of all possible sets of balancing parameters of the three cognates can be parametrized such that

1. The triangle of anchor point of balancing spring 1 (H) of the three cognates is proportional to the cognate triangle over the entire family. The two triangles are related by a combination of scaling, rotation and translation transformations.
2. The ratio of spring constant of balancing spring 1 (k_b) for the three cognates is the same throughout the one-parameter family. To calculate this ratio, the knowledge of location of the anchor point of the loading spring and the cognate triangle is enough.

It is believed that when an option of techniques 2 or 3 is being evaluated, the above parametrization would help a designer to better visualize balancing parameters of all the cognates in a unified manner. This result may be seen as extension of Roberts–Chebyshev cognate theorem to static balancing.

4. Discussion

In the static balancing techniques 1 and 2 as well as in options of technique 3 that has the same base for the balanced parallelogram and the plagiograph, one of the links pivoted to the ground does not play any role in static balancing. Link BC is such a link in Figs. 12, 16 and 17d. This link neither provides connection points to springs and auxiliary links nor influences the balancing parameters. If the link length is changed or the ground pivot of the link is changed or the link is altogether removed, the static balance remains unaffected. Consequently, these methods can be applied to spring-loaded serial two-revolute-jointed (2R) linkages also since removing a ground pivoted link from a four-bar linkage gives a 2R linkage.

Furthermore, when additional kinematic constraints are added to a linkage that is already in static balance, the static balance remains unaffected. Hence, loaded 2R linkage that is constrained as in a slider crank linkage is also amenable to the static balancing techniques of this paper.

Furthermore, in [6], it was shown that gravity loads are limiting cases of zero-free-length spring loads. Hence, the techniques of this paper are applicable even when zero-free-length spring loads are replaced by gravity loads.

Table 3
Ratio of spring constants of balancing spring 1 for three cognates.

Technique	$k_{b_1} : k_{b_2} : k_{b_3}$	$k_{b_1} : k_{b_2} : k_{b_3}$ rewritten using $W_1H_1 : W_2H_2 : W_3H_3 = W_1P : W_2P : W_3P$ or $1:1:1$
3	$\frac{k_l(L_1W_1)}{m_1^2(W_1H_1)} : \frac{k_l(L_2W_2)}{m_2^2(W_2H_2)} : \frac{k_l(L_3W_3)}{m_3^2(W_3H_3)}$ (see Eq. (7))	$\frac{(L_1W_1)}{m_1^2(W_1P)} : \frac{(L_2W_2)}{m_2^2(W_2P)} : \frac{(L_3W_3)}{m_3^2(W_3P)}$ or $\frac{(L_1W_1)}{m_1^2} : \frac{(L_2W_2)}{m_2^2} : \frac{(L_3W_3)}{m_3^2}$
2 Case *(ii)* of Section 3.1 applies	$k_l \frac{KW_1}{W_1H_1} : k_l \frac{KW_2}{W_2H_2} : k_l \frac{KW_3}{W_3H_3}$ (see Eq. (3))	$\frac{KW_1}{W_1K} : \frac{KW_2}{W_2K} : \frac{KW_3}{W_3K} = 1:1:1$ $\because$ K is the same as P in this case

5. Conclusions

In this paper, three techniques to statically balance a zero-free-length spring-loaded four-bar linkage were presented with the motivation that these could be the starting point for the design of statically balanced systems involving inherent and possibly more complex elastic loads. The only spring-load static balancing technique in the existing literature turned out to be a sub-option of one of these techniques. While the current approach in literature involves extending static balance of a skew lever to plagiograph, this paper's approach involves suitably composing the loading spring or its equivalent with another spring and then balancing the resultant spring by introducing a parallelogram linkage. The number of additional links and springs required for all these techniques is less than or equal to that of static balancing solution found in the existing literature. In terms of additional links that are added for balancing, a technique was singled out as the best since it does not require any auxiliary link. A prototype demonstrating this option was made.

A more general problem, where choosing a four-bar linkage is also at the discretion of the designer, was also considered. This led to a situation where the designer has to evaluate different options of the techniques presented in this paper on all cognates of a four-bar linkage having a suitable coupler curve. In order to aid the designer to better visualize the balancing parameters of all the cognates, a new parametrization of the family of all possible sets of balancing parameters of the three cognates was given where (1) the triangle of anchor points of corresponding balancing springs of the three cognates could be visualized as scaled, and/or rotated or translated copies of the cognate triangle, (2) the ratio with respect to each other of spring constants of the corresponding balancing springs of the three cognates is the same over the parametrization, and the ratio can be calculated from the cognate triangle and the anchor point of loading spring. This was proved using elementary geometrical constructions. The result may be seen as an extension of Roberts–Chebyshev cognate theory to static balancing.

Acknowledgment

Authors thank Professor Just Herder for his insightful comments on this manuscript.

Appendix A. Proofs regarding finding focal pivot

Appendix A.1. If $I_{a,b}$ and $I_{c,a}$ circles are coincident, then the given lines a, b and c has to be concurrent

In the following proof, a, b, c, $I_{a,b}$ and $I_{c,a}$ refer to their original position, i.e., before rotation by β. Fig. 28 shows $I_{a,b}$ and $I_{c,a}$ circles that are coincident. Also shown are lines a and b and their intersection point $I_{a,b}$. Point $I_{c,a}$ should lie on this circle since the circle is its locus. By the definition of $I_{c,a}$ as the intersection of c and a, it should also line on line a. Hence $I_{c,a}$ should lie on the intersection of the circle with the line a.

Since $I_{c,a}$ and $I_{a,b}$ circles, by definition pass through A and line a also by definition pass through A, A is always an intersection point between the line and the circle. The following types of intersection between the circle and line a are possible:

1. When $I_{a,b}$ is distinct from A, the line a intersects the circle at two distinct points: A and $I_{a,b}$, as shown in Fig. 28.
2. When $I_{a,b}$ coincides with A, the line a has to be tangent to the circle at A. (see the theorem in Appendix B).

In the first possibility, $I_{c,a}$ has to be either at $I_{a,b}$ or at A. If it is at A, then line a has to be tangent to the circle (see the theorem in Appendix B), which contradicts the earlier observation that line a intersects the circle at two distinct points. Hence, $I_{c,a}$ cannot be at A, and by elimination, it has to be at $I_{a,b}$. This implies that $I_{a,b}$ and $I_{c,a}$ coincide which further imply that a, b, and c are concurrent.

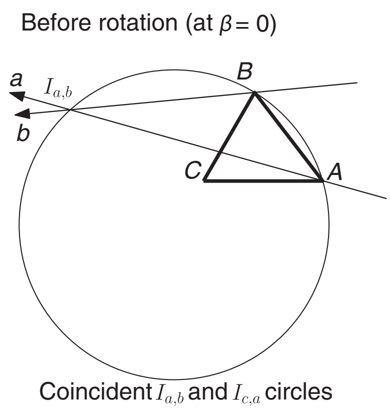

Fig. 28. $I_{a,b}$ and $I_{c,a}$ circles are coincident.

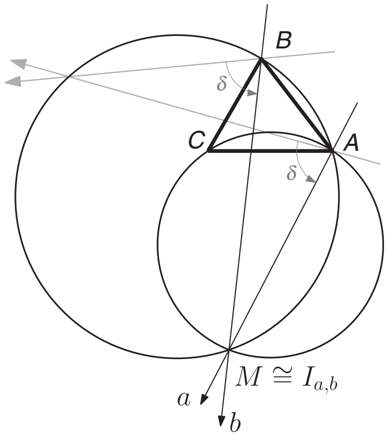

Fig. 29. $I_{a,b}$ is at *M*.

In the second possibility, since *A* is the only intersection between line *a* and locus of $I_{c,a}$, $I_{c,a}$ has be at *A*. Thus, here also both $I_{a,b}$ and $I_{c,a}$ coincide implying concurrence of lines *a*, *b* and *c*.

Hence, if $I_{a,b}$ and $I_{c,a}$ circles are coincident, then the given lines *a*, *b* and *c* has to be concurrent.

Appendix A.2. When M and A are distinct, M is the focal pivot (Refer to Section 3.1.4 and Fig. 27)

Let rotation angle β be such that point $I_{a,b}$ is at *A*, so that by the theorem in Appendix B, line *b* aligns along the segment *AB* and line *a* becomes tangent to $I_{a,b}$ circle. If for the same β, point $I_{c,a}$ is also at *A*, then by the theorem in Appendix B, line *a* becomes tangent to $I_{c,a}$ circle. This implies that line *a* is a common tangent to both $I_{a,b}$ and $I_{c,a}$ circles at the *A* which is one of the two distinct points of intersection of the two circles. This contradicts the fact that for two circles intersecting at two distinct points, there cannot be common tangent at the point of intersection. Hence there is no β for which both $I_{a,b}$ and $I_{c,a}$ are at *A*. Therefore *A* is not a focal pivot.

Let rotation angle β be such that $I_{a,b}$ is at *M* as shown in Fig. 29. It may further be seen that not only circle $I_{a,b}$ but even line *a* intersects the $I_{c,a}$ circle at two distinct points: *A* and *M*. Since point $I_{c,a}$ has to lie on both its locus $I_{c,a}$ circle and on line *a* (by definition), it should be at one of the intersection points (*A* or *M*) of the circle and the line.

If point $I_{c,a}$ is at *A*, then by the theorem in Appendix B, line *c* aligns with *CA* and line *a* becomes tangent to $I_{c,a}$ circle at *A*. This contradicts the earlier noted fact that line *a* intersects at two distinct points. Hence, point $I_{c,a}$ cannot be at *A* and by elimination of choices, it has to be at *M*. Thus, for the angle of rotation β, both $I_{c,a}$ and $I_{a,b}$ lie on *M*. Therefore, *M* is a focal pivot.

Appendix B. An elementary theorem of geometry

The angles subtended by a chord of a circle on any two points on the circumference of the circle are the same when the points are on the same side of the chord and are complement of each other when the points are on either side of the chord. The converse of the theorem is as follows: If two non-parallel lines passing through two ends of a line segment are rotated equally about the respective end-points of the segment, then the intersection point of the two lines traces a circle. The circle has the line segment as its chord. During rotation, when the intersection point reaches one end of the chord, one of the lines will align with the chord while the other becomes tangent to the circle.

References

[1] A. Agrawal, S.K. Agrawal, Design of gravity balancing leg orthosis using non-zero free length springs, Mechanism and Machine Theory 40 (2005) 693–709.
[2] D.J.B.A. de Lange, M. Langelaar, J.L. Herder, Design of a statically balanced compliant grasper using topology optimization, New York, paper number: DETC2008-49794, ASME International Design Engineering Technical Conferences, August 2008.
[3] E.A. Dijksman, Motion Geometry of Mechanisms, Cambridge University Press, ISBN: 0-521-20841-6, 1976.
[4] S. Hegde, G.K. Ananthasuresh, Design of single-input–single-output compliant mechanisms for practical applications using selection maps, ASME Journal of Mechanical Design 132 (August 2010) 081007-1–081007-8.
[5] J.L. Herder, Design of spring force compensation systems, Mechanisms and Machine Theory 33 (1) (1998) 151–161.
[6] J.L. Herder, Energy-free systems: theory, conception and design of statically balanced spring mechanisms, PhD dissertation, Delft University of Technology, ISBN: 90-370-0192-0, 2001.
[7] J.L. Herder, F.P.A. van den Berg, Statically balanced compliant mechanisms (sbcmâ€™s), an example and prospects, Baltimore, Maryland, paper number: DETC2000/MECH-14144, Proceedings ASME DETC 26th Biennial Mechanisms and Robotics Conference, September 2000.
[8] L.L. Howell, Compliant Mechanisms, John Wiley and Sons, Inc., 2001.
[9] L.L. Howell, A. Midha, Parametric deflection approximations for end-loaded, large-deflection beams in compliant mechanisms, ASME Journal of Mechanical Design 117 (March 1995) 156–165.
[10] K.H. Hunt, Kinematic Geometry of Mechanisms, Oxford University Press, Oxford, 1978.

[11] R.M. Nathan, A constant force generation mechanism, ASME Journal of Mechanisms, Transmissions, and Automation in Design 107 (4) (December 1985) 508–512.
[12] P. Pracht, P. Minotti, M. Dahan, Synthesis and balancing of cam-modulated linkage, Vol. 10 of The 1987 ASME Design Technology Conferences-The Design Automation Conferences, 1987.
[13] D.A. Streit, B.J. Gilmore, Perfect spring equilibrators for rotatable bodies, ASME Journal of Mechanisms, Transmissions, and Automation in Design 111 (4) (December 1989) 451–458.
[14] D.A. Streit, E. Shin, Equilibrators for planar linkages, ASME Journal of Mechanical Design 115 (September 1993) 604–611.
[15] D.C. Tao, Applied Linkage Synthesis, Addison-Wesley Publishing Company Inc., Reading MA, 1964.
[16] N. Ulrich, V. Kumar, Passive mechanical gravity compensation for robot manipulators, Proceedings of the 1991 IEEE International Conference on Robotics and Automation., April 1991, Sacramento, California.
[17] G.J. Walsh, D.A. Streit, B.J. Gilmore, Spatial spring equilibrators theory, Mechanism and Machine Theory 26 (2) (1991) 155–170.